Journal of Computational and Applied Mechanics, Vol. 2., No. 2., (2001) pp. 175–188

SUPPRESSION OF KÁRMÁN VORTEX EXCITATION OF A CIRCULAR CYLINDER BY A SECOND CYLINDER SET DOWNSTREAM IN CRUCIFORM ARRANGEMENT

Heon Meen Bae
National Fisheries Research and Development Institute
408-1 Shirang-Ri, Kijiang-Up, Kijiang-Kun, Pusan, 619-900 Korea

László Baranyi
Department of Fluid and Heat Engineering, University of Miskolc
H-3515 Miskolc-Egyetemváros, Hungary
arambl@gold.uni-miskolc.hu

Mizuyasu Koide
Department of Mechanical Engineering, Nagaoka University of Technology
Kamitomioka, Nagaoka, 940-2188 Japan
orange@stn.nagaokaut.ac.jp

Tsutomu Takahashi and Masataka Shirakashi
Department of Mechanical Engineering, Nagaoka University of Technology
Kamitomioka, Nagaoka, 940-2188 Japan
ttaka@mech.nagaokaut.ac.jp,kashi@mech.nagaokaut.ac.jp

[Received: July 26, 2001]

Abstract. A new technique for suppressing the Kármán vortex excitation of an elastically supported circular cylinder placed in an otherwise uniform flow is presented in this paper. By placing another cylinder downstream of it in a cruciform arrangement with a gap s between the two cylinders, the oscillation of the upstream cylinder can be virtually eliminated in the range of $\frac{s}{d_1} < 0.4$, where d_1 is the diameter of the upstream cylinder. Compared with conventional techniques, this offers the following advantages: i) it is unnecessary to change the shape of the oscillating body or remodel its supporting structure, and ii) the flow approaching the upstream body is practically undisturbed.

Keywords: Kármán vortex excitation, longitudinal vortex, circular cylinder, cruciform arrangement.

1. Introduction

When a cylindrical bluff body is exposed to a flow, vortices are shed from both sides of the body into the wake. This vortex shedding gives rise to a periodic lift force acting on the body. When the frequency of vortex shedding coincides with the natural frequency of the body, large amplitude oscillation or resonance can occur, Bearman [4]. This phenomenon is known as Kármán vortex excitation. This type of oscillation can be observed in many engineering practices, e.g., structures placed in the flow of air or a liquid, or flow around the tubes of heat exchangers and other

equipment. Due to its practical importance, much effort has been devoted to clarifying the mechanism of vortex excitation. This is of primary importance if one wishes to predict this phenomenon and to develop methods for suppressing or controlling the exciting forces, Sarpkaya [7], Parkinson & Wawzonek [6], Blevins [5].

Application of available techniques for reducing the amplitude of oscillation is limited since they require modifications of the oscillating body or that of its supporting structure. Hence there is a strong demand for a technique for controlling the Kármán vortex excitation without the need for changing the body or its supporting structure.

Inspired by the work of Tomita *et al.* [11,12] on the acoustic effect of a downstream cylinder, the present authors have found that the Kármán vortex excitation can be suppressed by a cylinder set downstream in cruciform arrangement, Shirakashi *et al.* [9], Bae *et al.* [1-3].

The specific aim of this work is to investigate the conditions needed to facilitate this suppression effect and to clarify its mechanism from a fluid dynamical point of view.

Notations

$\overline{C}_p$	time mean pressure coefficient, $\left(=\overline{p}/\frac{1}{2}\rho U^2\right)$
$\overline{C}_{pb}$	time mean base pressure coefficient
d_1	diameter of the upstream cylinder
d_2	diameter of the downstream cylinder
f_{nz}	natural frequency of the elastically supported (upstream) cylinder
f_{vK}	frequency of Kármán vortex shedding
f_z	frequency of cylinder vibration
k	spring constant of the elastically supported (upstream) cylinder
l	effective length of upstream cylinder (see Figure 1)
m	effective mass of upstream cylinder
p	static pressure
Re	Reynolds number $(=Ud_1/v)$
s	gap between the two cylinders (see Figure 1)
S_p	linear spectrum of the fluctuating pressure
S_{pp}	peak value in the linear spectrum of the fluctuating pressure
St	Strouhal number
S_u	linear spectrum of the velocity fluctuation
S_{up}	peak value in the linear spectrum of the fluctuating velocity
U	free stream velocity
u	velocity in x direction (see Figure 1)
z_{rms}	root-mean-square value of the displacement of the elastically supported (upstream) cylinder in z direction
α	angle measured from upstream stagnation point (see Figures 5 and 6)
δ	logarithmic damping factor
ν	kinematic viscosity of air
ρ	density of air

Subscripts

∞	for a single cylinder
L	left
r	resonance
R	right
rms	root-mean-square value
s	separation

Superscript

$-$	time mean value

2. Experimental apparatus and procedure

An outline of the experimental apparatus and coordinate system is shown in Figure 1. The wind tunnel is a blowdown type with a square nozzle measuring 350 mm x 350 mm. The maximum attainable velocity is 40 m/s and the turbulence intensity is less than 0.4%. The measuring channel is 320 mm x 320 mm in cross section and 1000 mm in length. The upstream circular cylinder which is supported elastically is set horizontally in the central plane of the test section, and it is allowed to move almost purely in the vertical (z) direction. Another circular cylinder is set vertically downstream of the horizontal cylinder with a gap s between them. The diameters of the upstream and downstream cylinders are d_1 and d_2, respectively. The aspect ratio of the upstream cylinder l/d_1 is about 12, which corresponds to the spanwise coherent length of a Kármán vortex.

The upstream cylinder passes through slots on the side walls of the test section, and is supported by two identical plate springs outside the side walls, Shirakashi et al. [8]. This setup allows a slight change of attack angle (rotation of the cylinder about its axis) to be superimposed on the z displacement of the cylinder. However, its influence on the oscillation of the circular cylinder is negligible since the length of the plate springs is very large compared with the oscillation amplitude and hence its maximum absolute value is very small. The end plates (shown in Figure 1) are installed in order to avoid flow through the slots. Thus the cylinder displacement is assured to be virtually purely translational in the vertical direction. The characteristics of the oscillating systems used in this experimental study are summarized in Table 1, where the effective mass m, the natural frequency f_{nz}, and the logarithmic damping factor δ are determined through a free damping oscillation in otherwise quiescent air.

The free stream velocity U was measured by a Pitot-static tube. Hot wire probes were used to detect the x component of the fluctuating velocity signals. The displacements at both ends of the upstream cylinder, z_L and z_R, were measured by using non-contacting sensors. Since z_L and z_R were identical under almost all experimental conditions, the motion of the cylinder was assumed to be purely translational. In this paper, the average of z_L and z_R is taken as the translational displacement of the cylinder, and the oscillation amplitude was represented by its root-mean-square value z_{rms}.

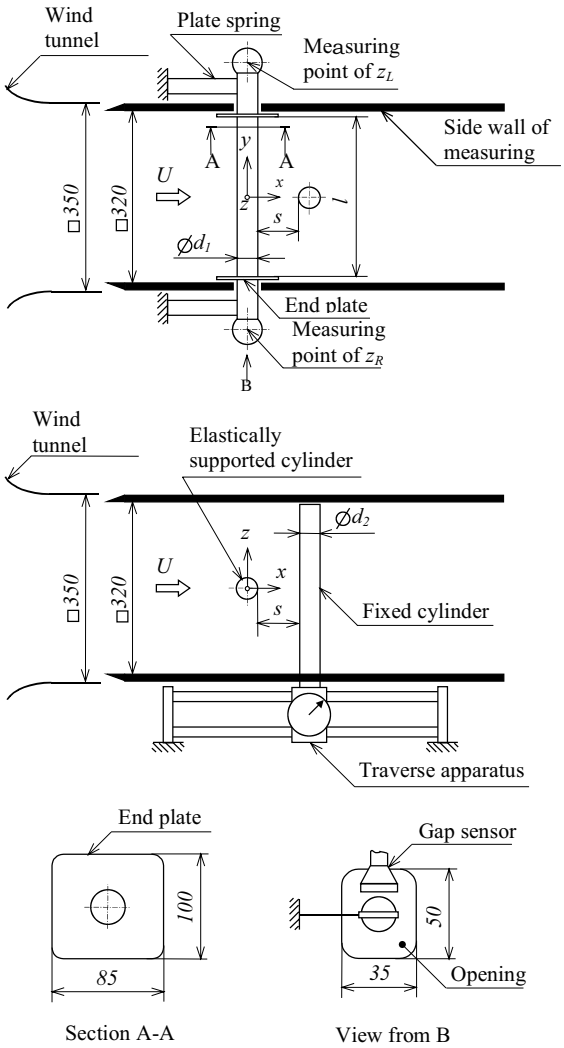

Figure 1. Outline of the apparatus with a coordinate system (unit in mm)

The pressure distribution on the surface of the upstream cylinder was measured with both upstream and downstream cylinders fixed. The geometry of the supporting system and that of the end plates were identical with the one used when the upstream cylinder is allowed to oscillate. The difference of the pressure on the upstream cylinder surface and the static pressure of the free stream was measured by using pressure taps of 0.4 mm in diameter on the surface of a hollow upstream cylinder made of acrylic resin and having a diameter of 26 mm. The hot wire probe was located downstream of the cylinders in a place where the spectrum of the fluctuating velocity signal had a sharp peak. The Kármán vortex shedding frequency f_{vK} was determined as the frequency at which the spectra of the velocity and pressure, S_u and S_p, both have peak values.

Table 1. Characteristics of the oscillating systems

	Oscillating system I	Oscillating system II
Upstream cylinder diameter: d_1 (mm)	26.0	26.0
Downstream cylinder diameter: d_2 (mm)	26.0	18.0 26.0 32.0
Effective length: l (mm)	304	304
Effective mass: m (kg)	0.0858	0.0924
Spring constant: k (N/m)	980	2100
Natural frequency: f_{nz} (Hz)	17	24
Logarithmic damping factor: δ $(-)$	0.0119	0.0166

In order to visualize the flow pattern on the cylinder surface, the oil-film method was used. A transparent vinyl film of 0.1 mm in thickness was rolled on the surface of the upstream cylinder, and the surface of this film was coated with a mixture of oil and matt-black paint. After having been exposed to the flow, the vinyl film roll was removed, and passing light from below the film made the flow pattern visible.

3. Results and discussion

3.1. Effect of free stream velocity on the vibration of the upstream cylinder. Figure 2 shows the variation of the Kármán vortex shedding frequency f_{vK}, the amplitude z_{rms}, and oscillation frequency of the cylinder f_z versus free stream flow velocity U. In Figure 2 quantities z_{rms}, f_z, and f_{vK} are made dimensionless by diameter d_1 and natural frequency f_{nz}, respectively. The Kármán vortex excitation for the single cylinder is clearly seen in Figure 2(a). However, when the downstream cylinder is added, although the Kármán vortex excitation peak appears at the same velocity, the excitation is substantially suppressed (see Figure 2(b)). It was found that the oscillation frequency coincided with the natural frequency, regardless of flow velocity U. In case of the single cylinder (Figure 2(a)), the amplitude z_{rms} has its maximum in a very small velocity interval at around 2.5 m/s. It is concluded from the results that this vibration is a typical resonance of a system with a small damping factor, i.e., Kármán vortex excitation. The resonance amplitude is denoted by $[z_{rms}]_r$. Narrowing the gap between cylinders reduces the Kármán vortex excitation substantially; in Figure 2(b), where the dimensionless gap $s/d_1 = 0.75$, the amplitude of vibration is reduced to one-fourth of that of the single cylinder.

3.2. Effect of the gap between cylinders on the amplitude of oscillation. Figure 3 shows the relationship between the amplitude of the Kármán vortex excitation $[z_{rms}]_r$ and the dimensionless gap s/d_1. The vertical bars show the range in oscillation amplitude. Results for downstream cylinders of different diameters are compared in this figure. It was found that $[z_{rms}]_r$ is almost independent of the diameter of the downstream cylinder for dimensionless gap values of $s/d_1 \geqslant 2$.

By bringing the downstream cylinder closer to the upstream one, the amplitude of oscillation of the two bigger cylinders decreases for $0.4 < s/d_1 < 2$, and it is suppressed completely for $s/d_1 \leq 0.4$. The region of s/d_1 with this complete suppression becomes wider with the increase of diameter d_2. As seen in Figure 3, when the diameter of the

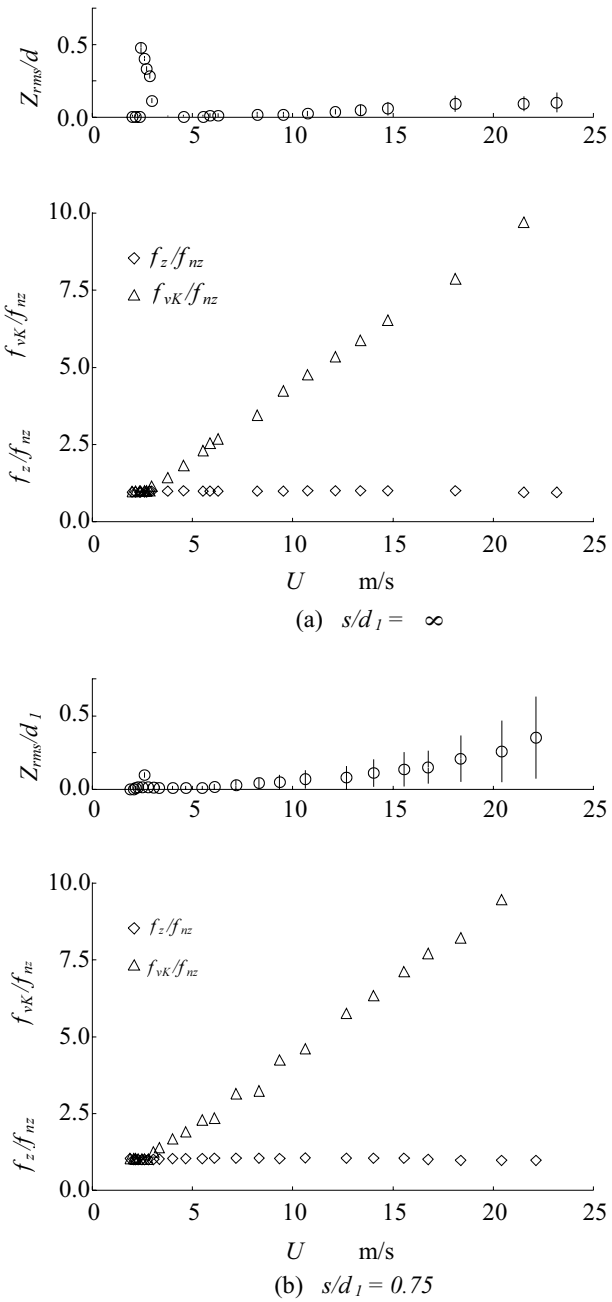

Figure 2. Variation of the nondimensional amplitude and frequency of vibration and the vortex shedding frequency with the freestream velocity (oscillating system I, probe position: $x/d_1 = 2.0;\ y/d_1 = 1.5;\ z/d_1 = 1.0;\ d_1 = d_2 = 26$ mm)

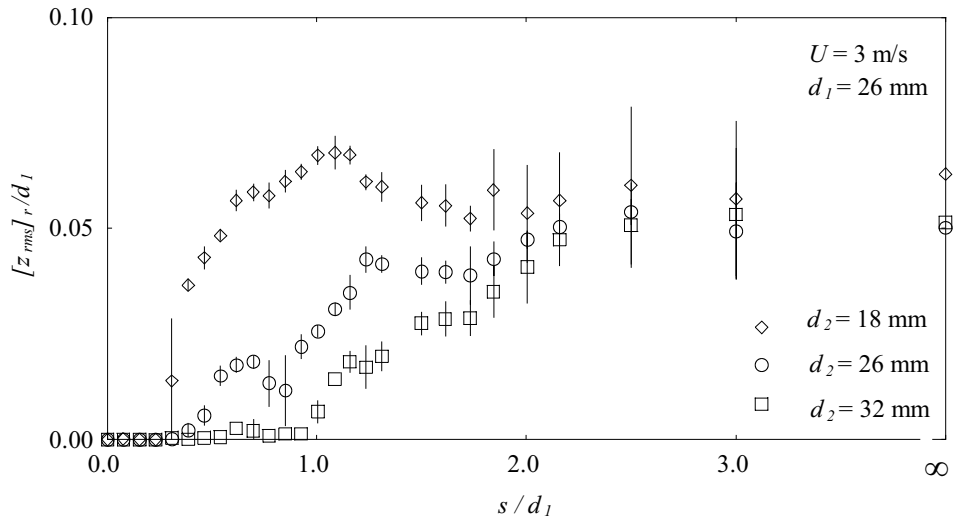

Figure 3. Variation of the vibration amplitude with the gap between two cylinders (oscillating system II)

downstream cylinder is smaller than that of the upstream one, i.e. at $d_2/d_1 = 0.69$, the amplitude of oscillation also becomes nearly zero for small enough gap values. This means that almost complete suppression of oscillation can be achieved for downstream cylinders of smaller diameters as well, but the range of s/d_1 for complete suppression becomes narrower.

3.3. Flow around the upstream cylinder. Flow around the upstream cylinder of the fixed system (i.e. both cylinders are fixed) was investigated to find the mechanism of the suppression of Kármán vortex excitation by the downstream cylinder. Figure 4 shows the flow pattern on the surface of the upstream cylinder visualized by the oil-film method for three different s/d_1 values. In Figure 4(a) which shows the case of $s/d_1 = 0$, the separation lines (indicated by arrows) are distorted into highly curved arcs for $|y/d_1| < 1.0$. The appearance of secondary flow in the wake behind the cylinder makes the oil-film pattern rather complex in this region. The separation lines outside of this region are almost straight lines parallel to the axis of the upstream cylinder. From now on the former region will be referred to as the primary effect region, and the latter as the secondary effect region. The length of the primary effect region along the axis of the cylinder depends on the nondimensional gap s/d_1*;* the region of primary effect scarcely appears on the oil-film for $s/d_1 > 1.0$.

The photographs in Figure 4 can be used for the determination of the relationship between the separation angle α_s (see Figure 5) and the dimensionless distance y/d_1 for different s/d_1 values. These relationships are shown and compared with the results of Tomita *et al.* [12]. The separation lines in the secondary effect region remain parallel with the axis of the cylinder for $y/d_1 > 4.0$, but the separation angle α_s is

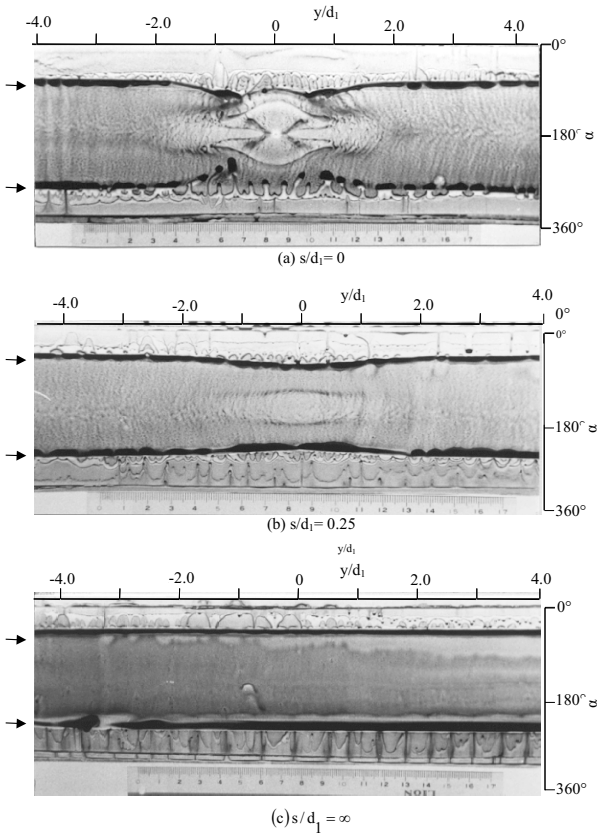

Figure 4. Flow visualisation on the surface of the upstream cylinder by the oil-film method (fixed system $d_1 = d_2 = 26\ mm$; $U = 8\ m/s$; $Re = 14700$; $\rightarrow$: separation line)

about 5 degrees smaller in this y/d_1 domain than the separation angle for the single cylinder. The distribution of the time mean pressure coefficient $\overline{C}_p$ on the surface of the upstream cylinder is shown in Figure 6 at cross sections, specified by various y/d_1 values. The distribution of $\overline{C}_p$ in the primary effect region of the cylinders in cruciform arrangement is notably different from the distribution around a single cylinder. On the other hand, the pressure distributions are almost the same for the secondary effect region with two cylinders and for the single cylinder. However, the pressure on the rear part of the upstream cylinder surface is a little higher than that on the single cylinder, and the separation line is found to move a little upstream in the former case. The effect of the downstream cylinder on the spectra of the fluctuating velocity and pressure S_u and S_p in the secondary effect region $y/d_1 > 4.0$ is shown in Figure 7. The measuring position was chosen as the one where the fluctuation component due to the Kármán vortices is most definitely observed. When the dimensionless gap $s/d_1 > 2.0$, the spectra S_u and S_p have sharp peaks at the frequency of $f = 24$ Hz. The Strouhal number for this frequency is $St = 0.2$, indicating that the sharp peaks

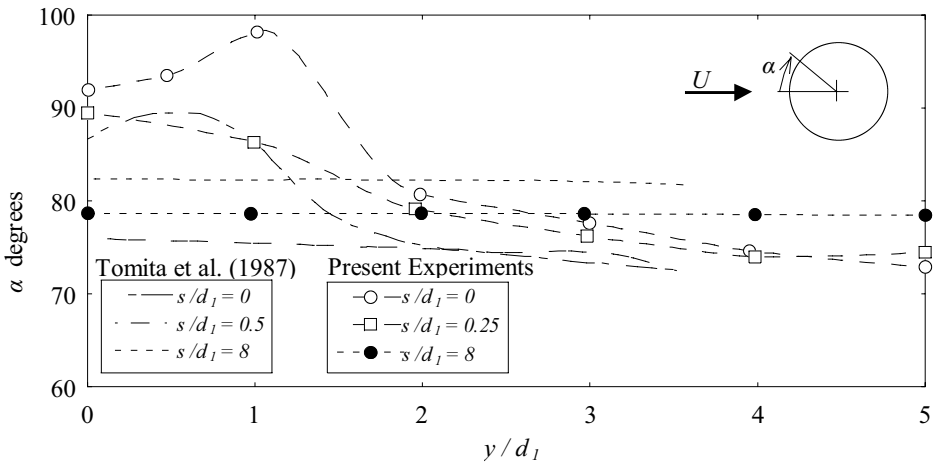

Figure 5. Variation of the separation angle with the spanwise coordinate y for different gap values (fixed system; (a) $d_1 = d_2 = 20\ mm$; $Re = 27000$; (b) $d_1 = d_2 = 26\ mm$; $Re = 14700$)

are caused by Kármán vortices. Although the decrease of the dimensionless gap s/d_1 reduces the magnitude of the height of spectral peaks S_{up} and S_{pp}, the frequency of Kármán vortex shedding f_{vK} remains unchanged. From the results above, the main features of the two regions for cylinders in cruciform arrangement can be summarized as follows:

1. The primary effect region: The mean flow field is very different from that of the single cylinder, and is strongly three-dimensional due to the influence of the downstream cylinder. Kármán vortex shedding is totally suppressed in this region.
2. The secondary effect region: The main flow field is basically two-dimensional in this region, and is nearly identical with that of the single cylinder. Nevertheless, the pressure on the rear surface of the upstream cylinder increases a little due to the effect of the downstream cylinder, and the separation lines move slightly upstream. While the fluctuating components of the velocity and pressure signals u and p induced by the shedding of Kármán vortices are reduced with a decreased gap between cylinders, the vortex shedding frequency is unaffected.

3.4. Mechanism for the suppression of Kármán vortex excitation. Considering the results given above, possible factors in the suppression of Kármán vortex excitation by setting a downstream cylinder in the flow can be stated as follows:

1. There is no Kármán vortex shedding in the primary effect region, leading to the reduction of the excitation force acting on the cylinder.
2. The strength of circulation of vortices and the regularity of vortex shedding are reduced in the secondary effect region.
3. The phase of the Kármán vortices, cut into two by the downstream cylinder, can differ on each side.

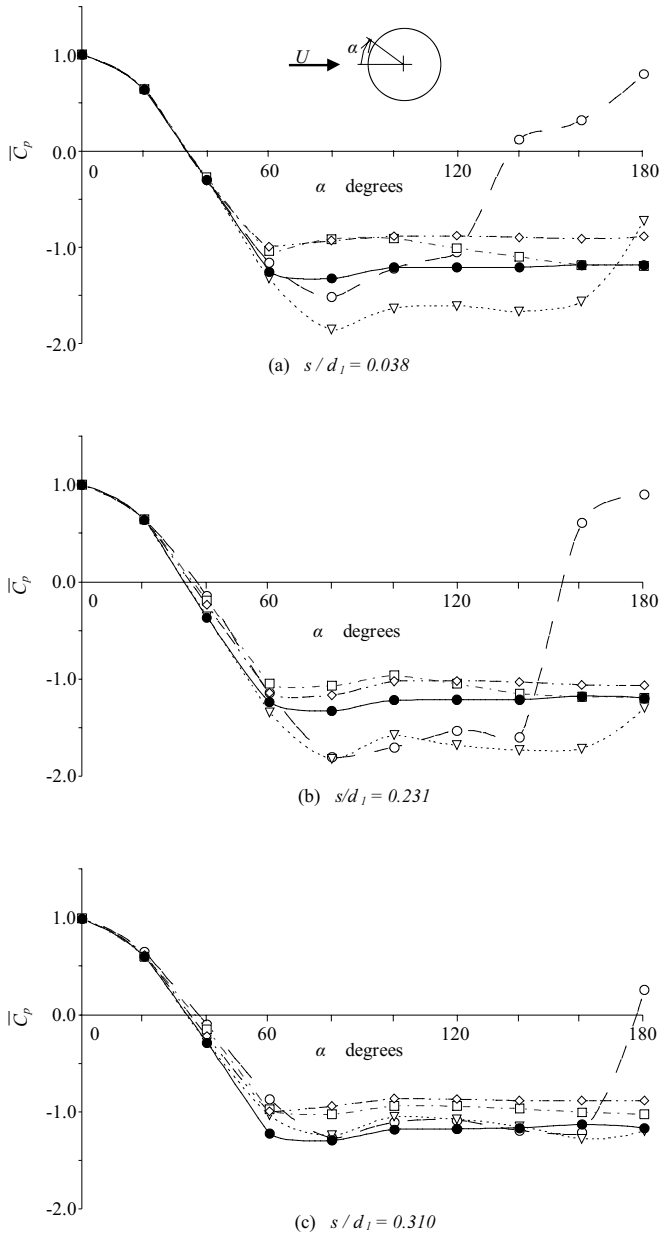

Figure 6. Pressure distribution on the surface of the upstream cylinder (fixed system; $d_1 = d_2 = 26\ mm$; $Re = 14700$; (o): $y/d_1 = 0.0$; (∇): $y/d_1 = 1.0$; ($\square$): $y/d_1 = 2.0$; ($\Diamond$): $y/d_1 = 3.0$; ($\bullet$): $y/d_1 = \infty$)

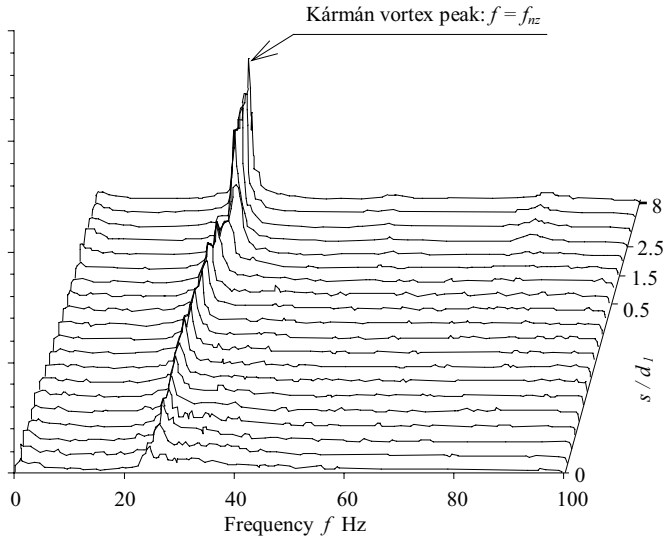

(a) The spectrum of the fluctuating velocity

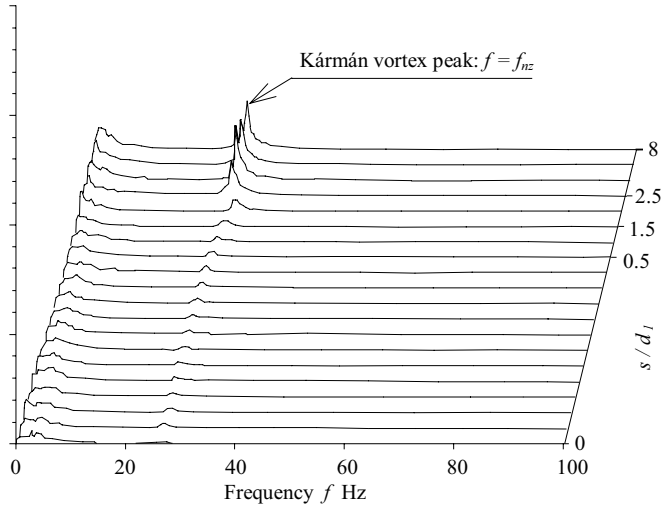

(b) The spectrum of the fluctuating pressure

Figure 7. Effect of the gap between the two cylinders on the spectra of the velocity and pressure at the point defined by the following coordinates: $x/d_1 = 2.0$; $y/d_1 = 4.0$; $z/d_1 = 2.0$; (fixed system; $d_1 = d_2 = 26$ mm; $Re = 5150$; pressure tap position: $\alpha = 80°$; $y/d_1 = 4.0$)

It is obvious that the reduction of the excitation force due to factor (1) is proportional to the ratio of the length of the primary effect region l_{sI} to the effective length of the upstream cylinder. The phenomenon, however, cannot be attributed solely to this cause, as it cannot explain why the amplitude of the upstream cylinder oscillation drops to almost zero for $s/d_1 < 0.4$ as found experimentally.

Factor (3) is based on the hypothesis that the correlation of the Kármán vortices, shed from the left and right parts of the horizontal upstream cylinder, becomes weaker since the downstream cylinder breaks the continuity of the Kármán vortex. Although this hypothesis may hold true for fixed upstream cylinders, such phase shift never occurs in an oscillating system because the Kármán vortex shedding synchronizes with the oscillation of the cylinder resulting in zero phase shift. Moreover there is some experimental evidence that even for fixed cylinders the pressure fluctuations due to Kármán vortex shedding in the secondary effect regions are in phase on each side of the downstream cylinder. Hence factor (3) is excluded as a possible cause of the suppression of vibration.

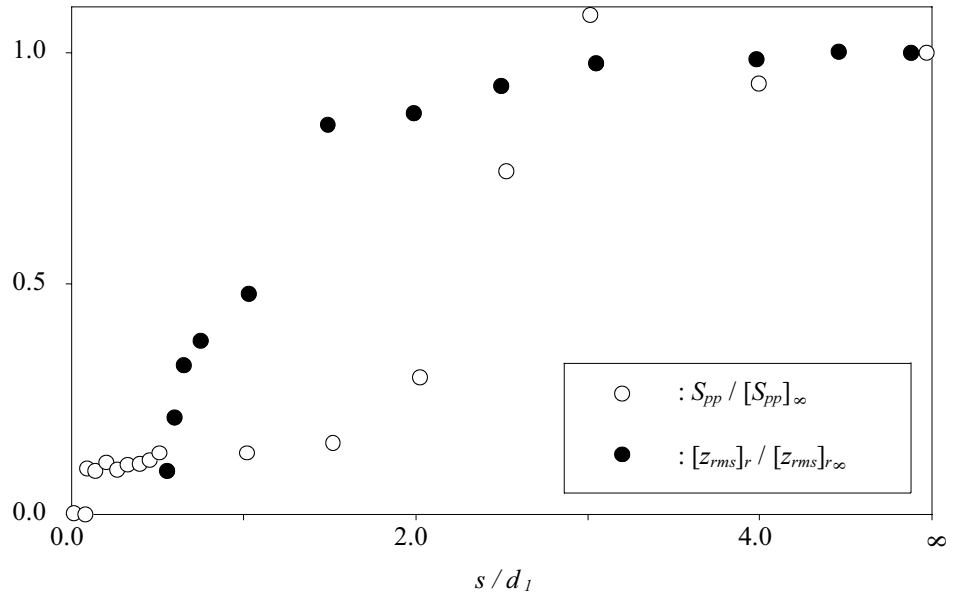

Figure 8. Variation of vibration amplitude and the spectral peak of pressure with the gap between the cylinders (fixed system; $d_1 = d_2 = 26\ mm$; $Re = 5150$; pressure tap position: $\alpha = 80°$; $y/d_1 = 4.0$)

The role of factor (2) is confirmed by looking into the correlation between the oscillation amplitude and the peak value of spectrum S_{pp} in the secondary region. The relationship between s/d_1 and the peak value S_{pp} of the pressure fluctuation spectrum is shown in Figure 8, and is compared with the Kármán vortex excitation amplitude $[z_{rms}]_r$.

The variables are made nondimensional by the corresponding values belonging to the single cylinder. The relationships between $S_{pp}/\,[S_{pp}]_\infty$ and s/d_1, further $[z_{rms}]_r\,/\,[z_{rms}]_{r\infty}$ and s/d_1 are similar to each other. The fact that S_{pp} is closely related to the fluctuating lift force acting on the cylinder at the frequency of f_{vK} (see Figure 8) suggests that factor (2) is one of the causes of the suppression of vibration.

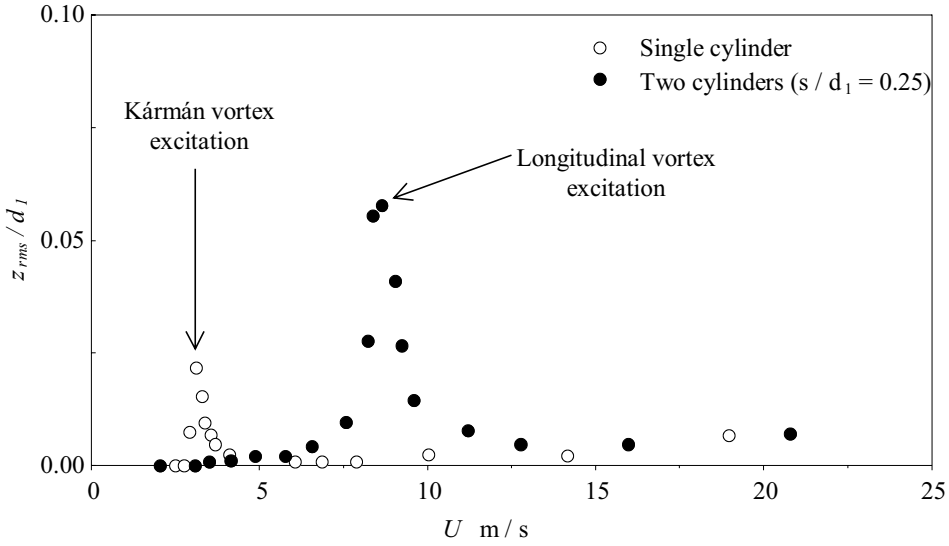

Figure 9. Longitudinal vortex excitation caused by the downstream cylinder

It should be noted that a large oscillation can be induced by the downstream cylinder. As seen in Figure 9, a high oscillation peak appears at a velocity three times higher than that of Kármán vortex excitation.

This oscillation is in resonance with the longitudinal vortices shed periodically near the crossing of the two cylinders, Shirakashi *et al.* [10]. Our investigations on this new excitation have shown that not only the velocity range of its occurrence, but also the phenomenon itself is completely different from those of the Kármán vortex excitation.

4. Conclusions

Kármán vortex excitation of an elastically supported circular cylinder placed in an otherwise uniform crossflow can effectively be suppressed by setting another cylinder downstream to it in a cruciform arrangement. Measurements of pressure on the upstream cylinder surface and velocity near the crossing, together with flow visualization, offer the following explanation for the phenomenon of suppression. Although the shedding frequency of Kármán vortices is unaffected by the downstream cylinder, the strength of circulation of a vortex is reduced and the periodicity of vortex shedding is disturbed along the whole span of the upstream cylinder due to the presence of the

downstream cylinder. In addition, there is no Kármán vortex shedding in the region near to the downstream cylinder.

The advantages of this technique are: i) it requires no modification in the shape of the oscillating body or in its supporting structure, and ii) the flow upstream of the oscillating body is virtually undisturbed.

REFERENCES

1. Bae, H.M., Arai, K., Roslin bin S. and Shirakashi, M.: *The influence of a cylinder located downstream on the oscillation of an elastically supported cylinder*, Proceedings of the 2^{nd} KSME-JSME Fluids Engineering Conference, Vol. 1, (1990), 72-77.
2. Bae, H.M., Baranyi, L., Takahashi, T. and Shirakashi, M.: *Suppression of Kármán vortex excitation of circular cylinders*, Proceedings of the 11^{th} Conference on Fluid and Heat Machinery and Equipment, Budapest, (1999), on CD ROM, 14/1-11.
3. Bae, H.M., Takahashi, T. and Shirakashi, M.: *Suppression of Karman vortex excitation of a circular cylinder by another cylinder located downstream in cruciform arrangement.* Bulletin of the JSME **59**, (557), (1993), 1-7.
4. Bearman, P.W.: *Vortex shedding from oscillating bluff bodies*, Annual Review of Fluid Mechanics **16**, (1984), 195-222.
5. Blevins, R.D.: *Flow-Induced Vibrations*, Van Nostrand Reinhold, 2^{nd} Edition, New York, 1990.
6. Parkinson, G.V. and Wawzonek, M.A.: *Some considerations of combined effects of galloping and vortex resonance*, Journal of Wind Engineering **81**(1-2), (1981), 135-143.
7. Sarpkaya, T.: *Vortex induced oscillations, A Selective Review*, Journal of Fluid Mechanics **46**, (1979), 241-258.
8. Shirakashi, M., Ishida, Y. and Wakiya, S.: *Higher velocity resonance of circular cylinder in crossflow*, Transactions of the ASME, Journal of Fluids Engineering, **108**, (1985), 392-396.
9. Shirakashi, M., Mizuguchi, K. and Bae, H.M.: *Flow-induced excitation of an elastically supported cylinder caused by another located downstream in cruciform arrangement*, Journal of Fluids and Structures **3**, (1989), 595-607.
10. Shirakashi, M., Bae, H.M., Sano, M. and Takahashi, T.: *Characteristics of periodic vortex shedding from two cylinders in cruciform arrangement*, Journal of Fluids and Structures, **8**, (1994), 239-256.
11. Tomita, Y., Inagaki, S., Suzuki, S. and Yokoyama, T.: *Acoustic characteristics of two circular cylinders forming a cross in uniform flow* (1^{st} Report, *Effect on noise reduction*), Bulletin of the JSME **29**(250), (1986), 1163-1170.
12. Tomita, Y., Inagaki, S., Suzuki, S. and Muramatsu, H.: *Acoustic characteristics of two circular cylinders forming a cross in uniform flow* (*Effect on noise reduction and flow around both cylinders*), JSME International Journal, **30**(265), (1987), 1069-1079.